Article:
Hernandez Aquino, R, Zaidi, SAR, McLernon, D et al. (1 more author) (2015) Energy Efficiency Analysis of Two-Tier MIMO Diversity Schemes in Poisson Cellular Networks. IEEE Transactions on Communications, 63 (10). pp. 3898-3911. ISSN 0090-6778

https://doi.org/10.1109/TCOMM.2015.2466534

Energy Efficiency Analysis of Two-Tier MIMO Diversity Schemes in Poisson Cellular Networks

Raul Hernandez-Aquino, Syed Ali Raza Zaidi, *Member, IEEE,* Des McLernon, *Member, IEEE,* and Mounir Ghogho, *Senior Member, IEEE*

***Abstract*—In this paper, the energy efficiency (EE) of different MIMO diversity schemes is analysed for the downlink of a two-tier network consisting of both macro- and femto-cells. The locations of the base stations (BSs) in both tiers are modeled by spatial Poisson Point Processes (PPPs). The EE of the system in b/J/Hz is obtained for different antenna configurations under various diversity schemes. Adaptive modulation is employed to maximize both the throughput and the EE across both tiers. Borrowing well established tools from stochastic geometry, we obtain closed-form expressions for the coverage, throughput and power consumption for a two tier rate adaptive cellular network. Building on the developed analytical framework, we formulate the resource allocation problem for each diversity scheme with the aim of maximizing the network-wide EE while satisfying a minimum QoS in each tier. We consider that both the number of antennas and the spectrum allocated to each tier constitute the network resource which must be efficiently selected for both tiers to maximize network-wide performance. The best performance in terms of the EE is provided by the schemes which strike a good balance between the achievable maximum throughput and the consumed power (both increasing with the number of RF chains used). In addition, the potential savings in EE by using femto-cells with sleeping mode capabilities are analysed. It is observed that when the density of active co-channel femto-cells exceeds a certain threshold, the EE of the system can be significantly improved by sleep scheduling.**

***Index Terms*—Energy efficiency, Rayleigh fading, MIMO, Poisson point process, spatial diversity.**

I. Introduction

A. Motivation

With the exponential increase in both the number of users of cellular systems and their bandwidth requirements, the typical approach of network designers has been to increase the data rates that the system can handle and improve the coverage where it is needed. However, until very recently designing for energy efficiency (EE) has not received the importance that it deserves in the development of techniques and algorithms for future wireless networks deployments. According to recent studies, around 2% of the CO_2 emissions to the atmosphere comes from the Information and Communication Technology (ICT) industry [1]. In particular, the share for telecommunications is around 1%, and this is directly related to the energy used in the cellular system. Moreover, about 80% of this energy is consumed by the Radio Access Network (RAN). So reducing the energy consumption in cellular networks has therefore both environmental and economical implications.

A promising solution for Next Generation Networks (NGNs) to cope with the demands for better coverage and higher data rates is through the deployment of heterogeneous networks (HetNets) which consist of smaller, cheaper and less energy consuming base stations (BSs) overlaid with the traditional macro BS network [2]. The use of HetNets has the potential to provide both the required coverage and increase the data rates of the users. However, realising such a potential may incur a significant energy penalty if the EE is not used as a metric to design the HetNet, mainly due to the increased co-channel interference.

Now, the use of MIMO technologies to improve communications performance has become a requirement for NGNs and it also has the potential to improve EE [3], [4]. However, the EE of the different MIMO techniques has not yet been analysed in depth, particularly beyond a point-to-point link. The use of multiple antennas has the direct benefit of increasing the average throughput. Nevertheless, the energy consumed also increases with the number of antennas, and this leads to a trade-off between throughput gains and the energy consumption. Additionally, the densification of the network to deal with traffic growth creates challenges for the efficient management of the available spectrum. While a co-channel deployment seems to be the appropriate choice when dealing with a relatively sparse network to avoid an underutilization of the spectrum, a disjoint channel assignment appears to be the best option for ultra dense deployment. Disjoint channel deployment of small cells has attracted support from 3GPP, whose Release 11 clearly identifies potential gains. Non co-channel deployment not only protects the users from the inter-tier interference but also provides a certain QoS guarantee. Such a deployment has been proposed by both academia [5] and industry [6]. NTT DOCOMO proposed the *phantom cell* concept, which advocates a deployment in which macro-cells manage the entire control plane, while the user plane is split between macro- and femto-cells [6]. Thus, users with high throughput requirements and low mobility can be served by femto-cells. While disjoint spectrum sharing between tiers seems to be the way ahead, the amount of spectrum shared across the tiers must be investigated. The optimal split of spectral resources is a function of various PHY layer param-

The authors would like to acknowledge the support from CONACYT, Mexico and US Army Research Lab Grant W911NF-13-1-0216.

This work was carried out with the support of Secretaria de Educacion Publica and the Mexican government.

R. Hernandez-Aquino, S.A.R. Zaidi and D. McLernon are with the School of Electronic and Electrical Engineering, University of Leeds, Leeds, United Kingdom. email: {elrha, s.a.zaidi,d.c.mclernon}@leeds.ac.uk

M. Ghogho is with the School of Electronic and Electrical Engineering, University of Leeds, Leeds, United Kingdom and also with the International University of Rabat, Morocco. email:{m.ghogho}@leeds.ac.uk

eters. Thus, the optimal allocation requires a characterization of the network wide performance in terms of these design parameters.To this end, the objective of this article is to investigate the design space of two tiered cellular networks where macro and femto-cells are deployed in non co-channel mode. Adaptive modulation is employed in each tier to maximize the attainable performance. BSs are equipped with multiple antennas to further enhance the downlink performance by exploiting the inherent diversity gain. The key objective of this study is to dimension the network-wide resource such that both EE and throughput can be maximized while satisfying some minimum desired QoS at each tier.

In order to characterize the performance of a large scale network, Poisson Point Processes (PPPs) [7] have frequently been used to model infrastructure-less networks such as ad-hoc [8]–[10] or femto-cell networks [11]–[14]. In these networks the randomness is an intrinsic ingredient of the network topology. Thus PPPs are a natural choice to capture the spatial dynamics. Furthermore, the use of PPPs has also been extended to model macro-cells [5], [15], [16], since the traditional hexagonal lattice based models only provide an upper bound on the performance of actual networks. Moreover the upper-bound comes at the cost of time consuming and tedious simulations and/or numerical integrations. In contrast, PPPs can accurately provide a lower bound on the network performance with an analytically tractable model. Therefore, in this work we make use of stochastic geometry tools to characterize the performance of various diversity schemes in terms of EE for a two tier network to find the diversity scheme and antenna configuration which provides the best performance. In order to characterize the coverage probability of each tier, the analysis carried out in [15], [17] is generalized and expanded. The optimum diversity scheme combinations along with the number of antennas are then obtained via a simple greedy search. We study both the case where only the energy related to the transmission is considered and the case which includes the total energy consumption (i.e., the energy used for signal processing, cooling, etc.). Finally, the impact of implementing sleep scheduling in the femto-tier is also investigated.

B. Related Work

There have been several works devoted to the study of the EE in heterogeneous networks, most of which consider an hexagonal grid for the modelling of the macro-cells positions. These provide an upper bound on the actual network performance but are unable to effectively produce a tractable framework from which aspects such as the scalability of the network can be evaluated. In [18] the EE gains were analysed by deploying micro-cells with fixed positions at the edge of a macro-cell network placed under the hexagonal lattice model. The area power consumption (defined as the amount of power used per unit area) was obtained as a function of the inter-site distance and it was found that there is an optimum value that minimizes this metric. A more general case was investigated in [19] where system throughput, area power consumption and EE were compared between a homogeneous network (only macro-cells deployed) and a heterogeneous network (consisting of both macro and micro-sites). In this case, the micro-cells were uniformly positioned near the border of each macro-cell, which accounts for a more realistic scenario, as the micro-cells will serve particular areas where the capacity or coverage needs to be improved, which will not necessarily only be at the edge of a macro-cell. In the case of femto-cell deployments, [20] addressed the compromise between spectral efficiency (or throughput) and EE for a two tier network consisting of macro-cells and a given number of femto-cells which are uniformly distributed inside the area of each macro-cell. Both tiers are assumed to operate with maximum ratio combining (MRC) as a diversity scheme and they share the same sub-channels for transmission. The results obtained show the degradation of the macro-cell throughput and the EE increment with an increasing number of femto-cells. Although the works described make use of realistic assumptions, the results were obtained mainly though simulations without providing an analytical framework.

Another trend found in recent works regarding the EE of wireless networks has been to make use of tools from stochastic geometry to characterize the performance of the networks with a tractable approach. The EE of a single-input single-output (SISO) two tier network consisting of both macro- and pico-cells was analysed in [21] where both tiers were modelled with independent PPPs. Analytical results on the coverage probability, data rates and EE (in bits/s/m $^{-2}$/J) were obtained as a function of the base station densities. Also, by considering independent PPPs, [22] evaluated the EE in a scenario consisting of micro-cells and pico-cells. An optimization problem was formulated to obtain the density of pico-cells that maximized the EE of the network with constraints on the outage probabilities of both tiers. The study of EE with the use of PPPs was extended to the multi-antenna case in [13], where a scenario consisting of a single macro-cell overlaid with a tier of femto-cells modelled with a PPP was analysed. The authors examined the throughput and the EE of a MIMO system with an opportunistic interference alignment scheme in order to mitigate interference. These works efficiently make use of PPP theory to obtain an analytical framework from which the EE of the network was evaluated. However, an open issue still remains when considering the EE aspects of antenna diversity schemes in the context of heterogeneous networks. In particular, the schemes which provide the highest gains in throughput may not necessarily be the ones which attain the highest EE, and so this is the focus of this work,

C. Contributions

In this paper, the EE of different MIMO diversity schemes is analysed for a two-tier network. In our previous work [23], we considered the EE aspect of Maximum Ratio Transmission (MRT). However, as the power used in the RF chains has a great impact in the overall EE of the network when multiple antennas are used (even more so than the power used for transmission) [24], in this work we further extend the analysis of EE to other diversity schemes where only some of the available antennas are used for transmission. Our main contributions can

now be summarized as follows. *Energy efficiency of MIMO diversity schemes*: The key aspect of this work is to analyse the performance of different MIMO diversity schemes from an EE point of view (in terms of bits/J/Hz). The schemes analysed in this work are: Joint Antenna Selection (JAS), Beamforming - Selection Combining (BF-SC) and MRT. Depending upon the number of antennas used, these schemes cover a wide range of other diversity schemes such as selection combining, maximum ratio combining or beamforming. In this regard, we address how the density of the femto-cells deployed in the network affects the EE for the different diversity schemes. It is worthwhile mentioning that diversity schemes with interferers modelled via a PPP were first analysed for ad-hoc networks in [17]. However, the authors focused on the scalability of the network in terms of transmission capacity and node density. Additionally, in the case of MRT the authors considered a bound on the maximum eigenvalue (of $\left(\mathbf{H}_i^{j,k}\right)^H \mathbf{H}_i^{j,k}$ - see later in this paper) in terms of the Frobenius norm. Here, we follow the approach in [25] which provides precise characterization[1].

Optimum diversity schemes and antenna configurations: We obtain the optimum diversity schemes and antenna configurations which yield the best performance in terms of EE for a given density of femto-cells deployed in the area. From this, we can address network design issues such as how the EE of the network is coupled with the number of antennas. Moreover, we deal with aspects such as whether it is more energy efficient to implement the same diversity schemes in both tiers and what antenna configuration will improve the EE metric in each case.

Adaptive modulation with MIMO: We consider the use of adaptive modulation in combination with MIMO spatial diversity to provide a model for practical systems which use a finite number of modulation schemes each of which corresponds to a finite number of possible constellation points.

Sleep mode: The effect of sleep mode with MIMO diversity schemes has not been investigated thoroughly in the context of two tier networks. In this work we analyse the savings when femto-cells are assumed to be able to go into sleep mode when they are not transmitting, thus effectively reducing the average energy used in the femto-cell tier while obtaining the same throughput, i.e. this enhances the EE.

D. Organization

The rest of the paper is organized as follows. Section II introduces the system model. The EE metric and its optimization are described in Section III. The expected throughput in each tier is derived in Section IV. Section V describes the analysis of the coverage for both tiers for the diversity schemes studied in this paper: JAS, BF-SC and MRT. The power consumption in the network is derived in Section VI. The simulation results are presented in Section VII. Finally, conclusions are given in Section VIII.

[1]Notice that the link success probability computed in [17] is a function of the transmitter-receiver association model. More specifically, in [17] the authors considered the well known bi-polar network model. However, for small cellular networks the performance must be averaged over the spatial distribution of the user.

Throughout the paper the following notation is used. Boldface capital and lower case letters represent matrices and vectors respectively. $E[X]$ stands for the expected value of the random variable X. $\mathbf{A}^H$ represents the conjugate transpose of the matrix $\mathbf{A}$. A random variable X following a complex Gaussian distribution with mean μ and variance σ^2 is expressed as $X \sim \mathcal{CN}(\mu, \sigma^2)$. $|\mathbf{A}|$ denotes the determinant of matrix $\mathbf{A}$, a_i denotes the i-th entry of vector $\mathbf{a}$ and $(\mathbf{A})_{l,n}$ denotes the (l,n)-th entry of matrix $\mathbf{A}$. Finally, an exponential distribution with mean μ is written as $\mathrm{Exp}\left(\frac{1}{\mu}\right)$.

II. System model

Consider the downlink of an interference limited OFDMA (such as LTE) two-tier network consisting of femto-cell access points (FAPs) and macro-cell base sations (MBSs). The effect of noise will be neglected as interference dominates the overall performance of the network. Note that this is the normal case for most modern cellular networks, where interference is the main performance limiting factor [15]. We focus on a highly dense scenario where both macro- and femto-cells always have a user to serve. We also assume that the total number of available subchannels (S) is divided between tiers, assigning orthogonal sub-channels to each one in a given time slot. So we will have $S_m < S$ sub-channels assigned to the macro-cell tier and $S_f = S - S_m$ sub-channels assigned to the femto-cell tier, such that the inter-tier interference is completely avoided, as the only sources of interference are base stations belonging to the same tier. As we are assuming a reuse factor of 1, all the cells in the network use the same sub-channels for transmission.

The propagation model is assumed to be a composite of Rayleigh flat-fading and path loss. For the flat fading component, a MIMO system is assumed where the base stations in tier i use M_i^t antennas for transmission and M_i^r antennas for reception. So, let $\mathbf{H}_i^{j,k}$ denote the $M_i^r \times M_i^t$ channel matrix between the j-th base station and the k-th user in tier i. As we consider a Rayleigh environment, each entry of $\mathbf{H}_i^{j,k}$ follows a complex Gaussian distribution with zero mean and variance 1, i.e., $(\mathbf{H}_i^{j,k})_{l,n} \sim \mathcal{CN}(0,1)$, with $l = 1, 2, ..., M_i^r$ and $n = 1, 2, ..., M_i^t$. We will model the path loss as $l(R_i^{j,k}) = \left(R_i^{j,k}\right)^{-\alpha_i}$, where $R_i^{j,k}$ is the distance from the j-th transmitter to the k-th user in tier i and α_i is the path loss exponent. In the femto-cell tier we use different values for the path loss exponent of the desired link (α_0) and the path loss exponent of an interferer link (α_f), as the later can experience different propagation scenarios [26]. The mean total transmitted power of a base station in tier $i \in \{f, m\}$ is denoted as P_i^{tx}, where "f"and "m" refer to "femto" and "macro", respectively. It is assumed that when a complex symbol $(s_i^{j,k})$ from the j-th transmitter to the k-th user is sent, then $E\left[\left|s_i^{j,k}\right|^2\right] = 1$.

Femto-cells are assumed to operate in closed subscriber mode [27], and so they will only serve their subscribed users. As femto-cell users are assumed to be located indoors, so a wall partition loss $(W_i,\ i \in \{f, m\})$ must be considered. This corresponds to the power which is lost when the RF signal

passes through a wall (for the macro-cell tier the users are assumed to be located outdoors, and so we consider $W_m = 1$). The tiers are modeled by two independent homogeneous PPPs $(\Phi_i,\ i \in \{f, m\})$ where the number of macro- and femto-cells in each tier are random variables following a Poisson distribution with positions uniformly distributed across the total area of the network. The intensity characterizing the number of base stations per unit area is λ_i. In the case of femto-cells, a Medium Access Probability (MAP) ρ_f is considered, where in the current time slot, each femto-cell decides whether to transmit (with probability ρ_f) or not. Therefore, the *effective intensity* of the transmitting femto-cells is given by $\rho_f \lambda_f$. The use of the MAP derives from the fact that the coexistence of femto-cells in the area of the network creates a need to control the co-channel interference, and this can be implemented by a MAP. It is worthwhile noting that a scenario in which femto-cells operate in CSMA/CA mode can be modelled by simply letting ρ_f be a function of a carrier sensing region, as in [28], [29]. To reduce interference, as in practial scenarios, macro-cells are assumed to be sectorized with N_S sectors and so the effective intensity of the interferers in this tier is considered to be $\frac{\lambda_m}{N_S}$[2]. In a highly dense scenario such as the one described, all sectors in a macro-cell are considered to be active but all of them use different subchannels, in order to effectively reduce the interference.

In the femto-cell tier each femto-cell user is assumed to be associated with a FAP, and its position randomly (uniformly) located in the coverage area of the femto-cell, which is assumed to the inside of a circle with radius R_c. Therefore, the distance of the user to its FAP ($R_f^{j,j}$) is a random variable with PDF $P_{R_f^{j,j}}(r) = \frac{2r}{R_c^2}$, for $0 < r \leq R_c$ [11]. On the other hand, in the macro-cell tier a user is associated with the closest BS, and this is the so called "closest association scheme" [15]. This means that $R_m^{j,j}$ is a random variable following the distribution of the distance to the closest base station, which for a homogeneous PPP was shown in [15] to be Rayleigh, i.e., $f_{R_m^{j,j}}(r) = e^{-\lambda_m \pi r^2} 2\lambda_m \pi r$, for $r \geq 0$. The scenario just described is depicted in Fig. 1(a) where both tiers can be observed. Note that under the closest association scheme used for the macro-cell tier, the cells form a Voronoi tesselation. In Fig. 1(b) the typical users of each tier are depicted, along with the distances to their associated base stations.

In the next section, the EE metric used is described and the main problem is clearly formulated.

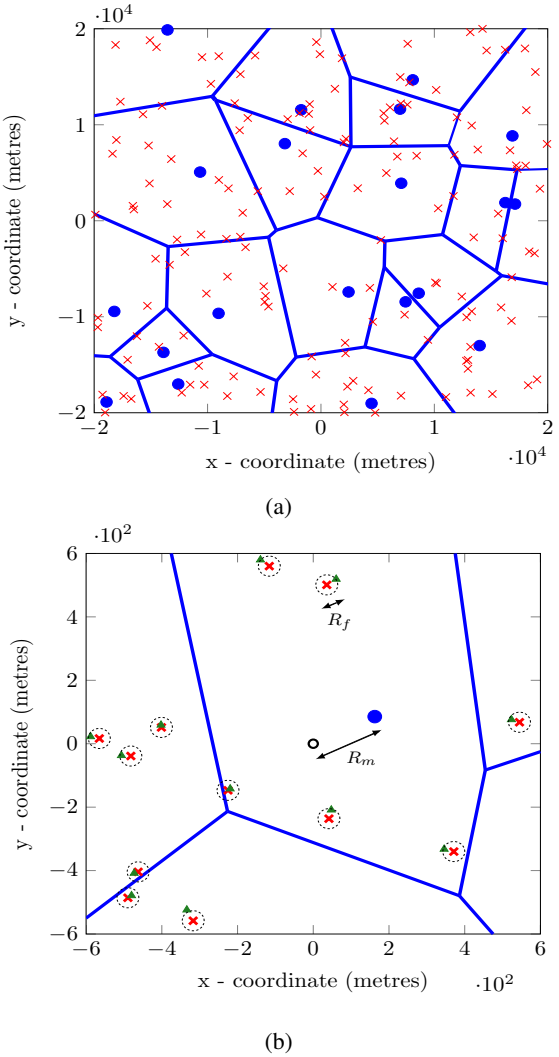

Fig. 1: (a) Two tier network consisting of femto-cells (red crosses) and macro-cells (blue dots). (b) the distance (R_m) of the macro typical user (black line circle) associated with its closest BS (blue dot) and the distance (R_f) of a femto user (green triangle) to its serving FAP (red cross). Note that each femto-cell is associated with a femto user which is considered to be uniformly distributed inside a circular area of radius R_c (dotted line) of the femto-cell.

III. Energy Efficiency

To characterize the EE of the system, we make use of the common metric defined in the Energy Consumption Rating (ECR) initiative [30], as

$$EE = \frac{T}{P} \text{ b/J} \tag{1}$$

where T is the effective throughput of the network in bps/Hz and P is the total power consumption in Watts. In order to obtain the EE of the diversity schemes studied in this work, we need to characterize both the total expected throughput of the network as well as the total power used.

The problem to be addressed in this work is an optimization problem where the optimum diversity scheme, as well as antenna configuration, is obtained for a given density of femto-cells deployed in the area, with QoS contraints. So, for each

[2]This holds for the downlink under the assumption that the front to back ratio of the sectorized antennas is high. In this case, the power radiated to a user in another sector can be neglected.

diversity scheme, the problem is defined as

$$M_i^{t\star}, M_i^{r\star}, S_m^{\star} = \arg \max_{M_i^t, M_i^r, S_m} \underbrace{\frac{S_m \lambda_m T_m + (S - S_m)\lambda_f T_f(\rho_f^{\star})}{\lambda_m P_m + \lambda_f P_f}}_{EE \text{ as in (1)}}$$

$$\text{s.t.}$$
$$S_m\, T_{m,u} \geq (S - S_m)\, q\, T_{f,u}\left(\rho_f^{\star}\right), \quad \text{if } T_{f,u}\left(\rho_f^{\star}\right) > T_{m,u}$$
$$(S - S_m)\, T_{f,u}\left(\rho_f^{\star}\right) \geq S_m q\, T_{m,u}, \quad \text{if } T_{f,u}\left(\rho_f^{\star}\right) \leq T_{m,u} \tag{2}$$

where T_m and T_f stand for (respectively) the expected throughput per base station in the macro- and femto-cell tier; $\rho_f^{\star}$ is the MAP value which maximizes the throughput in the femto-cell tier (see sections IV and V); u_i ($i \in \{f, m\}$) is the number of users served by each base station; $T_{m,u} = \frac{T_m}{u_m}$, $T_{f,u} = \frac{T_f\left(\rho_f^{\star}\right)}{u_f}$ are (respectively) the expected throughput experienced by a user in the macro- and femto-cell tier; P_m and P_f represent (respectively) the power consumed per MBS and FAP; and S_m is the number of subchannels assigned to the macro-cell tier. Additionally, $q \in [0, 1]$ is a quality of service requirement ensuring that a user in the tier with smaller throughput experiences at least a fraction (q) of the throughput of a user in the tier providing the highest throughput. The expression in (2) can be solved for $S_m^{\star}$ as a function of the other optimization variables ($M_i^{t\star}$, $M_i^{r\star}$) using the fact that the spectrum allocation is a linear combination with constraints on the minimum throughput requirement. Therefore, the EE would be maximized by assigning the maximum portion of the spectrum to the tier providing the highest EE, but the constraints set a limit on the spectrum allocated to the tier which experiences the lower expected throughput per user. The optimum value is then found when the constraints are met with equality, and is given by

$$S_m^{\star} = \begin{cases} S\left(1 + \frac{T_{m,u}}{q\, T_{f,u}\left(\rho_f^{\star}\right)}\right)^{-1} & \text{if } T_{f,u}\left(\rho_f^{\star}\right) > T_{m,u} \\ S\left(1 + \frac{qT_{m,u}}{T_{f,u}\left(\rho_f^{\star}\right)}\right)^{-1} & \text{if } T_{f,u}\left(\rho_f^{\star}\right) \leq T_{m,u}. \end{cases} \tag{3}$$

Now, both, the expected throughput and the power consumed depend on the diversity schemes and the number of antennas used in each case. These parameters need to be estimated in order to obtain the EE of the network in (2). We proceed to find expressions for the total expected throughput in section IV, which is a function of the coverage probability ($F^c_{SIR_i}(\beta_i)$, see section V). Then, we investigate the total power consumed in each tier in section VI.

IV. Network Throughput

In most modern wireless communication systems, the use of adaptive modulation according to the channel conditions has been used to maximize the throughput [32]. To the best of our knowledge no previous papers have studied adaptive modulation of MIMO diversity schemes with BSs deployed following a PPP. In this paper, we will further develop this scenario and study the performance of the diversity techniques under an adaptive modulation scheme for a two tier network. So, depending on the channel conditions, the symbols to be transmitted are chosen from a finite set of different constellations. Assuming R modulation schemes, in a given transmission then the normalized data rate that this system handles is given by $r_i^o = \log_2\left(1 + \frac{\beta_i^o}{G}\right)$ bps/Hz if $\beta_i^o \leq SIR_i < \beta_i^{o+1}$, with $o = 1, 2, ..., R$, $i \in \{f, m\}$ and G is the Shannon gap for un-coded QAM. In an adaptive modulation scheme, the average throughput per base station in each tier can be expressed as [32]

$$T_i = \sum_{o=1}^{R-1} r_i^o\, P\left(\beta_i^o < SIR_i \leq \beta_i^{o+1}\right). \tag{4}$$

Therefore, the total throughput in each base station for each tier is given by

$$T_m = \sum_{o=1}^{R-1} r_m^o \left(F^c_{SIR_m}(\beta_m^o) - F^c_{SIR_m}(\beta_m^{o+1})\right) + F^c_{SIR_m}(\beta_m^R) R$$
$$= \sum_{o=0}^{R-1} \left(r_m^{o+1} - r_m^o\right) F^c_{SIR_m}(\beta_m^{o+1}) \quad \text{bps/Hz/m}^2 \tag{5}$$

$$T_f\left(\rho_f\right) = \rho_f \sum_{o=0}^{R-1} \left(r_f^{o+1} - r_f^o\right) F^c_{SIR_f}(\beta_f^{o+1}) \text{ bps/Hz/m}^2 \tag{6}$$

where $F^c_{SIR_i}(x) = P(SIR_i > x)$ is the cumulative complementary distribution function (CCDF) of the SIR_i, and $r_m^0 = r_f^0 = 0$. Note that for the femto-cell tier, we have added the value of ρ_f, which accounts for the MAP of the femto-cell tier. This is due to the fact that ρ_f represents the percentage of

TABLE I: SIMULATION PARAMETERS (Similar to [18] and [31])

Parameter	Value	Description
R_c	30 m	Femto-cell coverage radius
α_m	4	Path loss exponent for the macro-cell tier
α_0	3	Path loss exponent for the femto-cell tier in the desired link
α_f	3.5	Path loss exponent for the femto-cell tier in an interference link
W_f	2, 4 dB	Wall partition loss for the femto-cell tier,
W_m	0 dB	Wall partition loss for the macro-cell tier
G	3 dB	Shannon gap
R	8	Number of constellations available
N_S	3	MBS antenna sectors
q	0.5	Quality of Service factor
u_m	30	Number of macro users per cell
u_f	2	Number of femto users per femto-cell
P_f^{tx}	100 mW	Femto-cell transmission power
P_m^{tx}	20 W	Macro-cell transmission power
a_f	4	Femto-cell power component dependent of transmitted power
a_m	3.77	Macro-cell power component dependent of transmitted power
b_f	9.6	Femto-cell constant power component
b_m	68.73	Macro-cell constant power component
P_{UE}^1	0.94 W	Power used at the receiver's UE when 1 RF chain is used for reception
P_{UE}^2	1.27 W	Power used at the receiver's UE when 2 RF chains are used for reception

time in which a femto-cell will be transmitting. The selection of MAP as the MAC strategy is justified given the fact that the femto-cells are limited in power, and so simpler algorithms are expected. Also, by having a MAP assigned, no power is expended for cooperation in the femto-cell tier.

As is clear from (5) and (6), we need to compute $F^c_{SIR_i}(\beta_i)$, defined as the coverage probability (which is formally described in the next section), in order to obtain the total throughput for each tier. The expression for the coverage probability is different between tiers and for different diversity schemes. In the next section, we examine the coverage probability for each of the schemes addressed in this work.

V. Coverage

The coverage probability of each tier $F^c_{SIR_i}(\beta_i), i \in \{f, m\}$ is defined as the probability that the received SIR is above a certain threshold (β_i), which depends on the required QoS (i.e., $F^c_{SIR_i}(\beta_i) = P(SIR_i > \beta_i)$). Next, the coverage is presented for the diversity schemes analysed in this paper. For convenience of notation, in the rest of the paper we drop the superscripts in the desired link, i.e. $\mathbf{H}_i = \mathbf{H}_i^{0,0}$, $R_i = R_i^{0,0}$ and $s_i = s_i^{0,0}$.

A. Joint Antenna Selection (JAS)

We first analyse the case of transmit antenna selection at the transmitter and selection combining at the receiver side, i.e., the transmitter and the receiver jointly select the link with the best instantaneous channel and so, only one antenna RF chain remains turned on (i.e., using energy) at both transmitter and receiver sides. In this scenario, there are $M_i^r M_i^t$ channels available, where each channel $(h_i(l,n))$ corresponds to each entry of the flat fading channel matrix, i.e. $h_i(l,n) = (\mathbf{H}_i)_{l,n}$, with $i \in \{f, m\}$, $l \in \{1, 2..., M_i^r\}$ and $n \in \{1, 2..., M_i^t\}$. The best channel ($h_i^\star$) is selected in this scheme, that is, it satisfies $h_i^\star = \max_{l,n} |h_i(l,n)|^2$. Using Slivnyak's theorem [15], without loss of generality we place a typical user at the origin and obtain its statistics. In this case, the received signal in the optimum link is given by

$$y_i = \sqrt{P_i^{tx}\, l\left(R_i\right)}\; h_i^\star s_i + \sum_{j \in \Phi_i} \sqrt{P_i^{tx}\; l\left(R_i^{j,0}\right) W_i^2}\; h_i^{j,0} s_i^{j,j} \tag{7}$$

where $h_i^{j,0}$ is the interfering channel coefficient corresponding to the link between the j-th transmitter and the desired user, for $i \in \{f, m\}$. From (7), the SIR can be computed as

$$SIR_i = \frac{|h_i^\star|^2\, R_i^{-\alpha_i}}{\sum\limits_{j \in \Phi_i} g^{j,0} W_i^2\, l\left(R_i^{j,0}\right)} = \frac{|h_i^\star|^2\, R_i^{-\alpha_i}}{I_{\Phi_i}},\;\; i \in \{f, m\} \tag{8}$$

where I_{Φ_i} corresponds to the interference due to the PPP Φ_i and $g^{j,0} = |h_i^{j,0}|^2$ represents the power of the channel between the j-th interferer and the desired user, with $g^{j,0} \sim \text{Exp}(1)$. The CCDF of $|h_i^\star|^2$ is obtained by using the fact that the CDF for an exponential random variable with mean equal to 1 is given by $F_X(x) = 1 - e^{-x}$, for $x \geq 0$. Thus, the CCDF $\left(F^c_{|h_i^\star|^2}\right)$, of the random variable $|h_i^\star|^2$, corresponding to the maximum value of $M_i^r M_i^t$ independent random variables, each one distributed as $\text{Exp}(1)$, is given by

$$\begin{aligned} F^c_{|h_i^\star|^2}(y) =& 1 - \left(1 - e^{-y}\right)^{M_i^r M_i^t} \\ =& \sum_{p=1}^{M_i^r M_i^t} \binom{M_i^r M_i^t}{p} (-1)^{p+1} e^{-py} \end{aligned} \tag{9}$$

where binomial expansion notation is used. Using (9) in (8), the coverage probability can be expressed as

$$\begin{aligned} & F^c_{SIR_i}(\beta) = P(SIR_i > \beta_i) \\ & = E_{I_{\Phi_i}, R_i}\left[\sum_{p=1}^{M_i^r M_i^t} \binom{M_i^r M_i^t}{p} (-1)^{p+1} e^{-s R_i^{\alpha_i} I_{\Phi_i}} \right]\Bigg|_{s = p\beta W_i^2} \\ & = \sum_{p=1}^{M_i^r M_i^t} \binom{M_i^r M_i^t}{p} (-1)^{p+1}\; E_{R_i}\left[E_{I_{\Phi_i}}\left[e^{-s R_i^{\alpha_i} I_{\Phi_i}} \right] \right] \\ & = \sum_{p=1}^{M_i^r M_i^t} \binom{M_i^r M_i^t}{p} (-1)^{p+1} \underbrace{E_{R_i}\left[\mathcal{L}_{I_{\Phi_i}}\left(s R_i^{\alpha_i}\right) \right]}_{\mathcal{K}_i(s, R_i)},\;\; i \in \{f, m\} \end{aligned} \tag{10}$$

where $\mathcal{L}_{I_{\Phi_i}}\left(s R_i^{\alpha_i}\right)$ corresponds to the Laplace transform of I_{Φ_i}. The resulting expressions for $\mathcal{K}_i(s, R_i)$ in each tier are given in the Appendix. Using these expressions, the formulas for the coverage in each tier are

$$\begin{aligned} & F^c_{SIR_m}(\beta) = \sum_{p=1}^{M_m^r M_m^t} \binom{M_m^r M_m^t}{p} (-1)^{p+1} \\ & \times \quad \left(1 + \left(\tfrac{p\beta\delta_m}{N_S(1-\delta_m)}\; {}_2F_1\left(1, 1-\delta_m; 2-\delta_m; -p\beta\right)\right)\right)^{-1} \end{aligned} \tag{11}$$

$$\begin{aligned} & F^c_{SIR_f}(\beta) = \\ & \sum_{p=1}^{M_f^r M_f^t} \binom{M_f^r M_f^t}{p} (-1)^{p+1}\; \frac{\gamma\left(\frac{\alpha_f}{\alpha_0}, R_c^{\alpha_0 \delta_f}\, \frac{\rho_f \lambda_f \pi^2 \delta_f}{\sin\left(\pi\delta_f\right)}\, (p\beta W_f^2)^{\delta_f}\right)}{R_c^2\, \frac{\alpha_0}{\alpha_f} \left(\left(\frac{\rho_f \lambda_f \pi^2 \delta_f}{\sin\left(\pi\delta_f\right)} \right)^{\alpha_f} (p\beta W_f^2)^2 \right)^{1/\alpha_0}} \end{aligned} \tag{12}$$

where $\delta_f = \frac{2}{\alpha_f}$, $\delta_m = \frac{2}{\alpha_m}$, and ${}_2F_1(a, b; c; x)$ is the hypergeometric function. Note that when $M_i^t = 1$ or $M_i^r = 1$, the expressions in (11) and (12) reduce (respectively) to the scenarios of a SIMO system performing selection combining at the receiver, or a MISO system selecting the best antenna at the transmitter.

B. Beamforming - Selection Combining (BF-SC)

In this scheme, beamforming is performed at the transmitter, while selection combining is performed at the receiver. The receiver selects the antenna, $\hat{l}$, with the largest value of $\|\mathbf{h}_i(l)\|^2$, out of the M_i^r possible branches, i.e., $\hat{l} = \arg\max_l \|\mathbf{h}_i(l)\|^2, l \in \{1, 2, ..., M_i^r\}$, where $\mathbf{h}_i(l)$ corresponds to the l-th row vector of $\mathbf{H}_i$, and only its corresponding RF chain remains turned on. Now, $\|\mathbf{h}_i(l)\|^2$ is a random variable which follows a χ^2 distribution with $2M_i^t$ degrees of freedom. We will denote as $\tilde{h_i} = \max_l \|\mathbf{h}_i(l)\|^2$, the random variable that corresponds to the maximum value among M_i^r random variables, each one χ^2 distributed and having $2M_i^t$ degrees of freedom. The information about the selected antenna at the receiver's side is fed back to the transmitter so that it can perform beamforming. Therefore, all RF chains remain on at

the transmitter side, while at the receiver only one RF is used. On the transmitter side, the complex symbol to be sent, s_i, is precoded before transmission with an $M_i^t \times 1$ beamforming vector, to give $\mathbf{v}_i\left(\hat{l}\right) s_i = \frac{\mathbf{h}_i^H(\hat{l})}{||\mathbf{h}_i(\hat{l})||} s_i$, $i \in \{f, m\}$. So the received signal (at the receiver's single antenna which remains turned on) is given by

$$\begin{aligned} y_i = &\sqrt{P_i^{tx}\, l\left(R_i\right)}\ \mathbf{h}_i\left(\hat{l}\right)\mathbf{v}_i\left(\hat{l}\right) s_i \\ &+ \sum_{j\in\Phi_i}\sqrt{P_i^{tx}\ l\left(R_i^{j,0}\right) W_i^2}\ \mathbf{h}_i^{j,0}\mathbf{v}_i^{j,j} s_i^{j,j} \end{aligned} \tag{13}$$

where $\mathbf{h}_i^{j,0}$ and $\mathbf{v}_i^{j,j} = \frac{\mathbf{h}_i^{j,j}}{||\mathbf{h}_i^{j,j}||}$ represent the j-th interference link channel vector and the beamforming vector in the j-th link, respectively, for $i \in \{f, m\}$. From (13), the SIR can be obtained as

$$SIR_i = \frac{\|\mathbf{h}_i(\hat{l})\|^2\, R_i^{-\alpha_i}}{\sum\limits_{j\in\Phi_i} g^{j,0} W_i^2\, l\left(R_i^{j,0}\right)} = \frac{\tilde{h_i}\, R_i^{-\alpha_i}}{I_{\Phi_i}},\ \ i \in \{f, m\}. \tag{14}$$

We use the fact that a linear combination of Gaussian random variables is also Gaussian, and so the power fading coefficients of the interferers $\left(g^{j,0}\right)$ follow an exponentially distributed random variable [17]. Now, the cumulative complementary density function, of the random variable $\tilde{h_i}$, can be expressed as [17]

$$\begin{aligned} F_{\tilde{h_i}}^c(y) &= 1 - \left(1 - e^{-y}\sum_{p=0}^{M_i^t-1}\frac{y^p}{p!}\right)^{M_i^r} \\ &= \sum_{w=1}^{M_i^r} e^{-wy} \sum_{p=0}^{M_i^r(M_i^t-1)} a_{wp}\, y^p \end{aligned} \tag{15}$$

where

$$a_{wp} = (-1)^{M_i^r+w}\binom{M_i^r}{w} \sum_{\substack{p_1,p_2,\ldots,p_w \le M_i^t-1 \\ p_1+p_2\ldots+p_w=p}} \prod_{v=1}^{w}(p_v!)^{-1},$$

and the sum runs over all ordered w-tuples of positive integers (including zero) less than $M_i^t - 1$ which add to p. Using (15), and the expression in (14), then the coverage can be expressed as

$$\begin{aligned} &F_{SIR_i}^c(\beta) = \\ &E_{I_{\Phi_i},R_i}\left[\sum_{w=1}^{M_i^r}\sum_{p=0}^{M_i^r(M_i^t-1)} a_{wp}\ e^{-w\beta W_i^2 R_i^{\alpha_i} I_{\Phi_i}} (\beta W_i^2 R_i^{\alpha_i} I_{\Phi_i})^p\right] \\ &= \sum_{w=1}^{M_i^r}\sum_{p=0}^{M_i^r(M_i^t-1)} \\ &\qquad a_{wp}\,(-1)^p\ \tfrac{\partial^p}{\partial w^p} E_{R_i}\left[E_{I_{\Phi_i}}\left[e^{-sR_i^{\alpha_i} I_{\Phi_i}}\right]\right]\Big|_{s=w\,\beta W_i^2} \\ &= \sum_{w=1}^{M_i^r}\sum_{p=0}^{M_i^r(M_i^t-1)} a_{wp}\,(-1)^p\ \tfrac{\partial^p}{\partial w^p}\ \underbrace{E_{R_i}\left[\mathcal{L}_{I_{\Phi_i}}(sR_i^{\alpha_i})\right]}_{\mathcal{K}(s,R_i)}. \end{aligned} \tag{16}$$

Using the expressions for $\mathcal{K}(R_i, s)$ presented in the Appendix, the coverage now becomes

$$\begin{aligned} F_{SIR_m}^c(\beta) = &\sum_{w=1}^{M_m^r}\sum_{p=0}^{M_m^r(M_m^t-1)} a_{wp}\,(-1)^p \\ &\times \tfrac{d^p}{dw^p}\left(1 + \left(\tfrac{w\,\beta\,\delta_m}{N_S(1-\delta_m)}\ {}_2F_1\left(1, 1-\delta_m; 2-\delta_m; -w\beta\right)\right)\right)^{-1} \end{aligned} \tag{17}$$

$$\begin{aligned} F_{SIR_f}^c(\beta) = &\sum_{w=1}^{M_f^r}\sum_{p=0}^{M_f^r(M_f^t-1)} a_{wp}\,(-1)^p \\ &\times \tfrac{\partial^p}{\partial w^p}\ \frac{\gamma\left(\frac{\alpha_f}{\alpha_0}, R_c^{\alpha_0\delta_f}\frac{\rho_f\lambda_f\pi^2\delta_f}{\sin\left(\pi\delta_f\right)}\,(w\beta W_f^2)^{\delta_f}\right)}{R_c^2\,\frac{\alpha_0}{\alpha_f}\left(\left(\frac{\rho_f\lambda_f\pi^2\delta_f}{\sin\left(\pi\delta_f\right)}\right)^{\alpha_f}(w\beta W_f^2)^2\right)^{1/\alpha_0}}. \end{aligned} \tag{18}$$

Note that by substituting M_i^t for M_i^r and vice-versa, the formulas obtained apply to a scenario now with antenna selection at the transmitter and MRC at the receiver (AS - MRC). Also, when $M_i^r = 1$, a pure beamforming scenario is addressed.

C. Maximum Ratio Transmission (MRT)

MRT consists of beamforming at the transmitter and MRC at the receiver [33]. Thus, in MRT scheme, all RF chains remain on at both transmitter, and receiver. The complex symbol to be sent, s_i, is first precoded at the transmitter with an $M_i^t \times 1$ beamforming vector $\mathbf{v}_i$, which is the eigenvector corresponding to the maximum eigenvalue (Λ_{max}) of the Wishart matrix $(\mathbf{H}_i)^H \mathbf{H}_i$. The received signal vector is then given by

$$\begin{aligned} \mathbf{y}_i = &\sqrt{P_i^{tx}\, l\left(R_i\right)}\ \mathbf{H}_i\mathbf{v}_i s_i \\ &+ \sum_{j\in\Phi_i}\sqrt{P_i^{tx}\ l\left(R_i^{j,0}\right) W_i^2}\ \mathbf{H}_i^{j,0}\mathbf{v}_i^{j,j} s_i^{j,j},\ \ i \in \{f, m\}. \end{aligned} \tag{19}$$

where $\mathbf{v}_i^{j,j}$ represents the eigenvector corresponding to the maximum eigenvalue of the Wishart matrix $\left(\mathbf{H}_i^{j,j}\right)^H \mathbf{H}_i^{j,j}$. At the receiver, MRC is used and a $1 \times M_i^r$ weight vector $(\mathbf{w}_i)^H$ is applied to the received signal before decoding the symbols, i.e., the signal to be decoded is given by $y_i = (\mathbf{w}_i)^H \mathbf{y}_i$, where $\mathbf{w}_i = \mathbf{H}_i\mathbf{v}_i$. The SIR in this case is given by

$$SIR_i = \frac{\Lambda_{max}\, R_i^{-\alpha_i}}{\sum\limits_{j\in\Phi_i} g^{j,0} W_i^2\, l\left(R_i^{j,0}\right)} = \frac{\Lambda_{max}\, R_i^{-\alpha_i}}{I_{\Phi_i}},\ \ i \in \{f, m\} \tag{20}$$

where $g^{j,0} \sim \text{Exp}(1)$ represents the fading power coefficient for the link between the desired user and the j-th source of interference. The SIRs in (20) follow from the fact that with MRC, the resulting interference is a weighted combination of complex Gaussian random variables, which is again Gaussian. This makes the power of the interference a sum of exponential random variables, just as in the case of a SISO system [25].

Now, from (20), this coverage probability is related to the CDF of the maximum eigenvalue (Λ_{max}) of a Wishart matrix, which was originally obtained in [34] as $F_{\Lambda_{max}}(x) = \frac{|\mathbf{\Psi}(x)|}{\prod_{k=1}^{t}(t-k)!\prod_{k=1}^{u}(u-k)!}$, where $t_i = \min\left(M_i^t, M_i^r\right)$, $u_i = \max\left(M_i^t, M_i^r\right)$ and $\mathbf{\Psi}(x)$ is a Hankel matrix whose elements are given by $\left(\mathbf{\Psi}(x)\right)_{i,j} = \gamma(i+j-1, x)$ with $\gamma(a, b)$ being the lower incomplete Gamma function. In [25] an alternative expression was found as a sum of exponential functions. Using this alternative expression ([25], eq. (15)) and applying the

definition in (20), the coverage probability is given as

$$F^c_{SIR_i}(\beta) = E_{I_{\Phi_i},R_i}\left[\sum_{p=1}^{t_i}\sum_{w=u_i-t_i}^{(u_i+t_i)p-2p^2}\sum_{z=0}^{w} d_{p,w} \times \frac{e^{-p\beta W_i^2 R_i^{\alpha_i} I_{\Phi_i}} (p\beta W_i^2 R_i^{\alpha_i} I_{\Phi_i})^z}{z!}\right]$$
$$= \sum_{p=1}^{t}\sum_{w=u_i-t_i}^{(u+t)p-2p^2}\sum_{k=0}^{w} d_{p,w}\frac{(-p)^z}{z!} \frac{\partial^z}{\partial p^z} E_{R_i}\left[E_{I_{\Phi_i}}\left[e^{-sR_i^{\alpha_i} I_{\Phi_i}}\right]\right]\Big|_{s=p\,\beta W_i^2}$$
$$= \sum_{p=1}^{t_i}\sum_{w=u_i-t_i}^{(u_i+t_i)p-2p^2}\sum_{z=0}^{w} d_{p,w}\frac{(-p)^z}{z!}\frac{\partial^z}{\partial p^z}\underbrace{E_{R_i}\left[\mathcal{L}_{I_{\Phi_i}}(sR_i^{\alpha_i})\right]}_{\mathcal{K}(s,R_i)} \tag{21}$$

where $d_{p,w}$ is a coefficient which can be obtained from $|\mathbf{\Psi}(x)|$ [25]. Using the expressions for $\mathcal{K}(R_i,s)$ presented in the Appendix, the coverage probabilities for each tier are given in (22) and (23).

By substituting the appropriate expressions for the coverage probability in each tier (as stated in the previous section) into (5) and (6) respectively, the throughput for each tier can be obtained. Depending on the particular scenario there is an optimal MAP value $\left(\rho_f^\star\right)$ which maximizes the throughput of femto-cells, i.e., $\rho_f^\star = \arg\max_{\rho_f} T_f(\rho_f)$. The expressions for the coverage probability in the femto-cell tier preserve the exponentially decreasing shape as a function of ρ_f (because of the Gamma function), while the multiplication by the linear increasing factor ρ_f means that the resulting expressions have an ALOHA like shape. This is shown in Fig. 2 of Section VII, where, depending upon the density of femto-cells, there is an optimum value for ρ_f. Unfortunately, the optimum MAP cannot be obtained in closed form expression, given the fact that the summations in (12), (18) and (23) are not known in theory. However, the MAP value can be computed by extending the summations for each configuration of antennas, then taking the derivative of (6), equating to zero and solving for $\rho_f = \rho_f^\star$, with the restriction that the resulting value is between 0 and 1. This can be carried out with the aid of a symbolic software program like Maple.

VI. Network power

We make use of the power consumption model presented in [18], [19], [35] for both macro and femto-cells: $P_i = a_i P_i^{tx} + b_i, i \in \{f,m\}$. Here a_i is a parameter dependent on the transmitted power of the base station (P_i^{tx}), which is related to the efficiency of the power amplifier, and b_i is a parameter independent of the transmission power which deals with the power used for signal processing, cooling effects of the site and battery backup. A power penalty for the CSI acquisition is not considered, as the transmitters in both tiers only require the channel information of the desired link which needs only a small number of bits to be fed back to the transmitter. We also assume typical values for the components of the power consumption model ([18], [31]) as presented in Table I.

Most of the works related to EE, only consider the power consumed at the transmitter side when analysing the downlink of a communication system [21], [22], [36], [37]. However in this paper, we also consider the power consumed at the User Equipment (UE), given the fact that not taking this power into consideration would result in an unfair comparison of the models when different numbers of antennas are assumed at the receiver. In [38], an analysis was carried out for the case of a system using the 802.11n standard for transmission (which is also used by several smartphones) and the mean power consumed was obtained using a Network Interface Card (NIC) when up to 3 antennas were used for reception. These values are presented in Table I, under the parameter $P_{UE}^{M_i^r}, i \in \{f,m\}$. Note that "$UE$" stands for User Equipment. By using the models previously described, the macro- and femto- tier total power consumption models per base station are given by

$$P_m = N_S\left(a_m P_m^{tx} + \bar{M}_m^t b_m\right) + P_{UE}^{\bar{M}_m^r} \quad \text{W} \tag{24}$$

$$P_f = \rho_f^\star a_f P_f^{tx} + \bar{M}_f^t b_f + P_{UE}^{\bar{M}_f^r} \quad \text{W} \tag{25}$$

where $\bar{M}_i^t$ and $\bar{M}_i^r$ represent the effective number of antennas (RF chains) used depending upon the diversity scheme. Namely, for MRT $\bar{M}_i^t = M_i^t, \bar{M}_i^t = M_i^r$, for BF-SC $\bar{M}_i^t = M_i^t, \bar{M}_i^t = 1$, and for JAS $\bar{M}_i^t = \bar{M}_i^t = 1$. Note that $a_i, i \in \{f,m\}$ in (24) and (25) are not scaled by the number of antennas, given that the total power radiated from all the antennas is equal to P_i^{tx}.

By substituting the values for T_i and P_i ($i \in \{f,m\}$) into (2) we can obtain the EE metric for each diversity scheme analysed. Now, from the expressions for coverage probability previously derived, the optimization problem in (2) is intractable for different values of M_i^t and M_i^r ($i \in \{f,m\}$). However, as we are dealing with a finite search space, we resort to an extensive search over the optimizing variables to obtain the results.

A. Sleep Mode

One of the techniques from which further improvements can be obtained in the power savings of a communications system is through the use of sleeping modes, as highlighted in [1], [36]. In a sleeping mode, a component of the communication system can be partially or completely shut down when its full operation is not justified. The use of sleeping modes in this work fits naturally in the context of the femto-cell MAP. Before sending information, each FAP decides individually whether to transmit (with probability ρ_f) or not (with probability $1-\rho_f$). If a FAP decides that it is not going to transmit in the current time slot, then there is a potential saving in the power used if this femto-cell can shut down its operation during the duration of the time slot.

Considering FAPs with sleep mode capabilities and neglecting the power consumed in a FAP when it goes into sleep mode (perfect sleep mode), then (25) becomes

$$P_f = \rho_f^\star\left(a_f P_f^{tx} + \bar{M}_f^t b_f\right) + P_{UE}^{\bar{M}_f^r} \quad \text{W}. \tag{26}$$

The improvements in the EE of the network with the use of femto-cell sleeping mode are presented in the next section. It is worthwhile mentioning that we are not considering the small energy which is used in switching from sleep to active mode, but it could easily be incorporated into the calculations.

$$F^c_{SIR_m}(\beta) = \sum_{p=1}^{t_m} \sum_{w=u_m-t_m}^{(u_m+t_m)p-2p^2} \sum_{z=0}^{w} d_{p,w} \frac{(-p)^z}{z!} \frac{d^z}{dp^z} \left(1 + \frac{p\,\beta\,\delta_m}{N_S\,(1-\delta_m)}\ {}_2F_1\,(1, 1-\delta_m; 2-\delta_m; -p\beta)\right)^{-1} \tag{22}$$

$$F^c_{SIR_f}(\beta) = \sum_{p=1}^{t_f} \sum_{w=u_f-t_f}^{(u_f+t_f)p-2p^2} \sum_{z=0}^{w} d_{p,w} \frac{(-p)^z}{z!} \frac{d^z}{dp^z} \frac{\gamma\left(\frac{\alpha_f}{\alpha_0}, R_c^{\frac{2\alpha_0}{\alpha_f}} \frac{\rho_f \lambda_f \pi^2 \delta_f}{\sin(\pi\delta_f)}\ (p\beta W_f^2)^{\delta_f}\right)}{R_c^{2\,\frac{\alpha_0}{\alpha_f}} \left(\left(\frac{\rho_f \lambda_f \pi^2 \delta_f}{\sin(\pi\delta_f)}\right)^{\alpha_f} (p\beta W_f^2)^2\right)^{1/\alpha_0}}. \tag{23}$$

TABLE II: DIVERSITY SCHEMES ANALYSED

Macro-cell scheme	Femto-cell scheme
MRT	MRT
JAS	JAS
MRT	BF - SC
BF - SC	MRT
BF - SC	JAS
JAS	BF - SC
MRT	JAS
JAS	MRT
BF - SC	BF - SC
JAS - MRC	JAS - MRC

VII. Results

Simulation results are now presented in Figs. 2 to 6 for both Monte-Carlo simulations (i.e., circles, with 2 x10^4 runs for each point) and the analytical plots (i.e., the lines). Note that the simulations lie (almost exactly) on the analytical plots. The parameters used for the simulations are given in Table I and we deliberately chose them similar to other publications [18], [11]. Given the fact that the user equipment is comprised of battery limited devices, the scenarios simulated in this work consider a maximum of $M_i^r = 2$ antennas per user, whereas the number of antennas in the BSs can be up to $M_m^t = 4$ in the macro-cell tier, and $M_f^t = 3$ for FAPs. In the simulations, we analysed different combinations of the diversity schemes previously described in each tier to obtain the optimum values of EE in each case. For all the diversity schemes and configurations we allocated the optimum portion of spectrum ($S_m^\star$) and for femto-cells we use the optimum value of the MAP ($\rho_f^\star$) in order to obtain the higher gains in throughput. Without loss of generality, in the simulations we have assumed that there are $R = 8$ integer available data rates (i.e., $r_i^1 = 1$, $r_i^2 = 2$,...,$r_i^8 = 8$, $i \in \{f, m\}$). All the combinations of the diversity schemes analysed are presented in Table II.

In Fig. 2 the throughput of the femto-cell tier is presented as a function of the MAP (ρ_f) for the main diversity schemes analysed, and with different values of the wall partition loss W_f. It can be seen that there is an optimum value ($\rho_f^\star$) that maximizes the throughput, and this varies depending upon the interference experienced. With a fixed density of femto-cells deployed in the area, a higher value of W_f translates into a smaller interference experienced in the desired link, and so, the optimum MAP $\rho_f^\star$ has a higher value. On the other hand, a small value for W_f represents a higher interference, and so $\rho_f^\star$ is smaller.

In Fig. 3, we present a comparison between the achievable

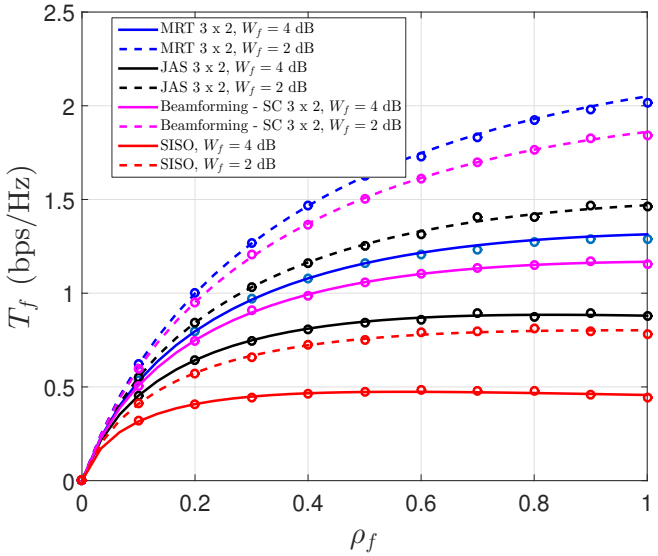

Fig. 2: Femto-cell throuhgput for the diversity schemes as a function of MAP (ρ_f). Circles represent Monte-Carlo simulations and lines represent analytical results.

EE when different diversity schemes are used in the femto-cell tier. In order to clarify the comparison, we kept the same diversity scheme and antenna configuration in the macro-cell tier, i.e. MRT with $M_m^t = 4, M_m^r = 2$. On the other hand, in the femto-cell tier we show a contrast between different diversity schemes and antenna configurations. The results obtained help us to gain some insight in the inherent tradeoff of throughput and EE. For example, while using MRT at the femto-cell tier would result in the highest achievable throughput for femto-cell users, a scheme with JAS outperforms MRT in terms of EE for the same number of antennas ($M_f^t = 3, M_f^t = 2$ in this case). Given that in a JAS scheme there will only be one RF chain left turned on at the transmitter and receiver whereas in MRT all the RF chains remain on, the results show that selectively keeping just a few chains for transmission generates higher gains on the overall EE. Therefore, a tradeoff between the throughput and the power of the system is evident. Moreover, we also observe that the EE achieved with a MRT scheme with $M_f^t = 3, M_f^t = 2$ in the femto-cell tier is actually inferior to the SISO case. Additionally, we note that a simple MRC in the femto-cell tier (MRT with $M_f^t = 1$) can actually outperform a MRT with multiple antennas at the FAP (MRT with $M_f^t > 1$). This result not only reinforces the previous statement about the gains in EE due to savings in energy resulting from the use of less RF chains, but also shows that

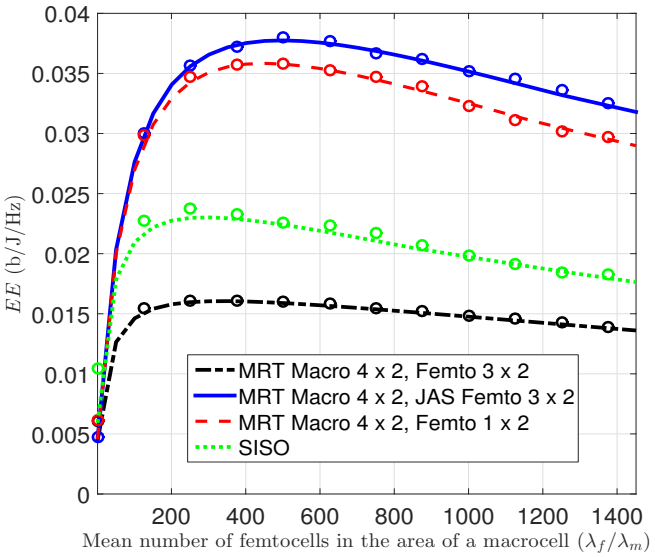

Fig. 3: Comparisons of diversity schemes and antenna configurations for the EE (see EE in (2)) versus average number of femto-cells in the area of a macro-cell $\left(\frac{\lambda_f}{\lambda_m}\right)$ with $b_f \neq b_m \neq 0$ in (24) and (25) (i.e., both transmit power and other sources included). Circles represent Monte-Carlo simulations and lines represent analytical results.

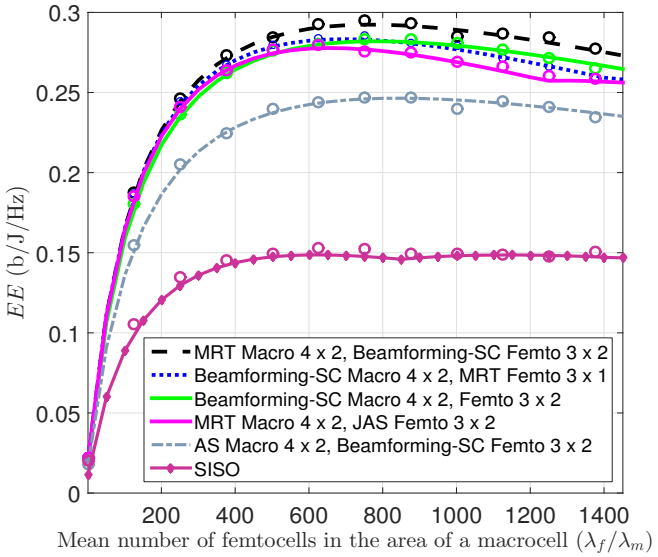

Fig. 4: Energy efficiency (see EE in (2)) versus average number of femto-cells in the area of a macro-cell $\left(\frac{\lambda_f}{\lambda_m}\right)$ with $b_f = b_m = 0$ in (24) and (25) (i.e., only transmit power considered). Circles represent Monte-Carlo simulations and lines represent analytical results. (Note that table II shows all the posibilities that we have examined but only schemes with the most significant results are presented in the graphs - similar for the rest of figures).

not all MIMO schemes achieve gains over a SISO case and the antenna configuration needs to be carefully selected for different combinations of diversity schemes.

In Fig. 4 the EE of the system is presented when only the power related to transmission is considered at the transmitter (i.e., $b_f = b_m = 0$ in (24) and (25)). This scenario is important when the main concern in the system is the amount of transmit power radiated at the transmission side. The plots presented correspond to some of the schemes yielding the best performance (given all the possible schemes from table II) and the SISO case is included for comparison purposes. It can be seen that increasing the number of available antennas at the transmitter side (for both macro- and femto-cells) has the direct effect of increasing the EE in most of the configurations. So regardless of the number of femto-cells deployed, the use of more antennas is usually desirable at the transmitter side. Additionally, the diversity schemes that provide the better results are the ones that use a higher number of the available antennas (from all those available), e.g. MRT (in which all RF chains are used), BF-SC (where all RF chains at the transmitter are used, while at the receiver only one RF remains turned on) and their combinations. In contrast, diversity schemes involving JAS (in which only one RF chain remains on at transmitter and receiver side) do not achieve the best performance in these scenarios. This can be understood intuitively, given the fact that by fixing the same amount of transmitted power for all configurations, the gains in throughput also account for higher gains in EE.

In Fig. 5 the EE of the system is obtained when we consider the total power (i.e., transmit power plus all other power components) at the transmitter side. The configurations with the highest achieved EE, along with results for a SISO system, are all presented. It can be seen that the increase in the number of femto-cells increases the EE of the system up to a certain threshold, after which the energy consumed by the femto-cells outweighs the gain in throughput, thus reducing the overall EE. We observe that, when the mean number of femto-cells deployed in the area of a macro-cell is approximately below 390, the best performance in EE is provided by a system with AS-MRC at both the macro-cell and femto-cell tier with $M_m^t = 4$, $M_m^r = 2$ and $M_f^t = 3$, $M_m^r = 2$. However, when the mean number of femto-cells exceeds this value, a system with MRT at the macro-cell tier ($M_m^t = 4$, $M_m^r = 2$) and JAS at the femto-cell tier ($M_f^t = 3$, $M_f^r = 2$) shows better results. These results show that the savings in power by not using all the RF chains is more beneficial to the EE than the gains in throughput obtained when all chains remain on. This is in contrast to the case when only the power used for transmission was considered. Moreover, for each antenna configuration there is a mean number of femto-cells which maximizes the EE of that configuration. From the results we also observe that in the femto-cell tier, the power consumed in the RF chains has a greater effect on the total EE compared to the increased gains in throughput resulting from using all the RF chains. That is, the gains in throughput obtained have much lesser impact on the EE than the total power used when a higher number of antennas (and their respective RF chains) are employed.

In Fig. 6 the improvements in the EE of the network can be observed when the femto-cells are equipped with sleep mode capabilities (using (26)). The schemes which provided the highest gains in EE at high femto-cell density are presented. It can be seen that the results can be divided into three regions.

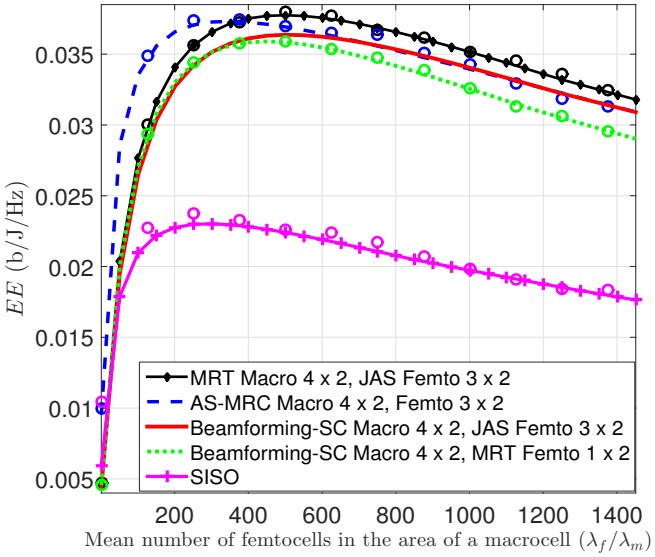

Fig. 5: Energy efficiency (see EE in (2)) versus average number of femto-cells in the area of a macro-cell $\left(\frac{\lambda_f}{\lambda_m}\right)$ with $b_f \neq b_m \neq 0$ in (24) and (25) (i.e., both transmit power and other sources included). Circles represent Monte-Carlo simulations and lines represent analytical results.

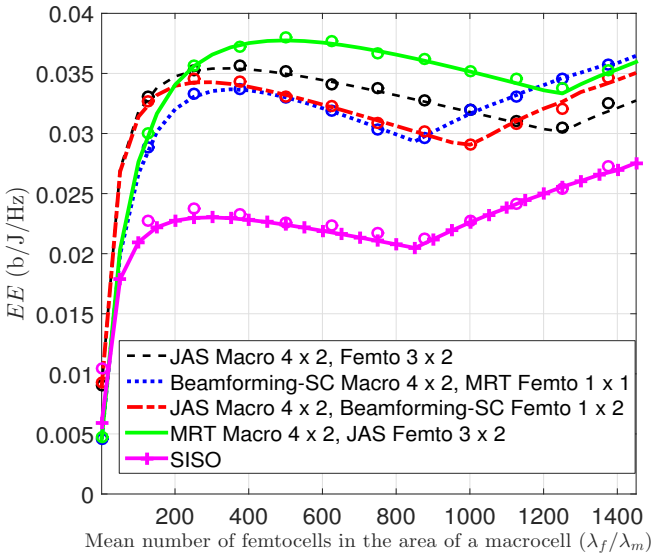

Fig. 6: Effect of incorporating sleep mode on the EE (using (26)) versus average number of femto-cells in the area of a macro-cell. Circles represent Monte-Carlo simulations and lines represent analytical results.

In the first region, the number of femto-cells deployed is small enough so that the interference in this tier is low and deploying more femto-cells is directly reflected in an increase in the EE of the system, up to a maximum value where the interference dominates the gains in throughput. In the second region, the increase in the number of femto-cells creates high interference in the tier, and so, the power consumed by the FAPs starts outweighing the increase in throughput, and the overall EE starts to decrease. Finally, there is a third region, in which the interference is still high and so there is not a lot of gain in the throughput, but the number of femto-cells which start to go into sleep mode is higher, and the power savings associated with this boosts the overall EE of the system. It is interesting to see that the results can provide insight into two main behavioural parts: the diversity scheme (and antenna configuration) dominating part, and the sleep mode dominating part. It can be concluded that for relatively small interference in the femto-cell tier, the highest gains in EE of the system come from the particular diversity scheme selected and the number of antennas used. Alternatively, for high interference, the savings in power consumption by using sleep mode have a bigger impact on the EE of the system than the achievable gains of the diversity schemes.

VIII. Conclusions

In this work, the achievable EE was obtained for different MIMO diversity schemes in a two tier network consisting of macro-cells and femto-cells. The optimal diversity schemes and antenna configurations were obtained for realistic parameters found in practice, and as we vary these parameters, (e.g., propagation exponent, wall partition loss and MBS density) the optimal configurations vary as well. The results illustrate the tradeoff between the energy consumption and the performance expected in terms of overall throughput. We observe that in general, for the macro-cell tier a higher number of antennas is normally desirable, regardless of the diversity scheme used. Additionally, the best performance in EE comes for a combination of different diversity schemes in the macro- and femto-cell tier, along with their respective optimum antenna configurations.

Results also show that when only the RF transmission power is considered for the EE, the use of a larger number of antennas (on both femto-cell and macro-cell downlink) increases the EE of the network (assuming the same transmitted power in all antenna configurations). Moreover, in this scenario diversity schemes using more RF chains such as combinations of MRT and BF-SC have the best performance. Alternatively, when other contributions to the overall network power consumption are also considered, a direct increase in the number of antennas can reflect gains in the EE, but the antenna configuration must be carefully selected in order to obtain gains in EE with respect to a SISO system. Furthermore, the optimal diversity schemes are normally the ones in which not all the antennas (and their respective RF chains) are used, such as combinations of BF-SC and JAS. Further improvements in the EE of the system were observed by equipping femto-cells with sleeping mode capabilities directly related to the medium access probability. We noted that there exists a threshold for the number of femto-cells which can be deployed in the network. Below this threshold, the best performance in EE comes by having all the femto-cells transmitting and the diversity schemes are the dominating factor. Alternatively, above this threshold some femto-cells can be shut down, effectively increasing the EE and the sleep mode then becomes the dominating factor for the overall EE of the system. This latter case applies to scenarios with high traffic loads.

APPENDIX A
EVALUATION OF $\mathcal{K}_i(s, R_i)$ IN (10)

For the femto-cell tier, the Laplace transform, is directly found in [8] as

$$\mathcal{L}_{I_{\Phi_f}}(sR_f^{\alpha_0}) = \exp\left(-\frac{\rho_f \lambda_f \pi^2 \delta_f}{\sin(\pi\delta_f)}\left(sR_f^{\alpha_0}\right)^{\delta_f}\right) \tag{27}$$

with $\delta_f = \frac{2}{\alpha_f}$. As was stated in the system model, the user is uniformly distributed in the area inside a radius R_c, and so we have

$$\begin{aligned}\mathcal{K}_f(s, R_f) =& E_{R_f}\left[\mathcal{L}_{I_{\Phi_f}}\left(sR_f^{\alpha_0}\right)\right] \\ =& \int_0^{R_c} \frac{2R_f}{R_c^2}\, e^{-\frac{\rho_f \lambda_f \pi^2 \delta_f}{\sin(\pi\delta_f)}\left(sR_f^{\alpha_0}\right)^{\delta_f}} dR_f. \end{aligned} \tag{28}$$

By using the substitution $u = \frac{\rho_f \lambda_f \pi^2 \delta_f}{\sin(\pi\delta_f)}\left(sR_f^{\alpha_0}\right)^{\delta_f}$ and the definition of the lower incomplete Gamma function $\gamma(a,x) = \int_0^x t^{a-1}e^{-t}dt$, we obtain

$$\mathcal{K}_f(s, R_f) = \frac{\gamma\left(\frac{\alpha_f}{\alpha_0}, R_c^{\frac{2\alpha_0}{\alpha_f}} \frac{\rho_f \lambda_f \pi^2 \delta_f}{\sin(\pi\delta_f)} s^{\delta_f}\right)}{R_c^2 \frac{\alpha_0}{\alpha_f}\left(\left(\frac{\rho_f \lambda_f \pi^2 \delta_f}{\sin(\pi\delta_f)}\right)^{\alpha_f} s^2\right)^{1/\alpha_0}}. \tag{29}$$

For the macro-cell tier, we have

$$\begin{aligned}\mathcal{K}_m(s, R_m) =& E_{R_m}\left[\mathcal{L}_{I_{\Phi_m}}\left(sR_m^{\alpha_m}\right)\right] \\ =& E_{R_m}\left[E_{I_{\Phi_m}}\left[e^{-sR_m^{\alpha_m} I_{\Phi_m}}\right]\right] \\ =& E_{R_m}\left[E_{\Phi_m, h^{j,0}}\left[e^{-sR_m^{\alpha_m}\sum\limits_{j\in I_{\Phi_m}} h^{j,0}\, l\left(R_m^{j,0}\right)}\right]\right] \\ =& E_{R_m}\left[\left[E_{\Phi_m}\prod_{j\in I_{\Phi_m}} E_h\left[e^{-sR_m^{\alpha_m} h\left(R_m^{j,0}\right)^{-\alpha_m}}\right]\right]\right] \\ =& E_{R_m}\left[E_{\Phi_m}\left[\prod_{j\in I_{\Phi_m}} \frac{1}{1+sR_m^{\alpha_m}\left(R_m^{j,0}\right)^{-\alpha_m}}\right]\right]. \end{aligned} \tag{30}$$

Using the definition of the generating functional and the substitution $u = \left(\frac{R_m^{j,0}}{R_m s^{\frac{1}{\alpha_m}}}\right)^2$, the resulting expression can be written as [15]

$$\mathcal{K}_m(s, R_m) = E_{R_m}\left[\exp\left(\frac{-\lambda_m \pi R_m^2}{N_S}\underbrace{s^{\delta_m}\int_{s^{-\delta_m}}^{\infty}\frac{du}{1+u^{\frac{1}{\delta_m}}}}_{\zeta(s,\alpha_m)}\right)\right] \tag{31}$$

where $\delta_m = \frac{2}{\alpha_m}$. Now, the binomial negative series expansion is defined as

$$(a+x)^{-n} = \sum_{k=0}^{\infty}(-1)^k\binom{n+k-1}{k}x^k a^{-n-k}. \tag{32}$$

Applying the definition in (32) to $\zeta(s,\alpha_m)$ in (31), with $a = u^{\frac{1}{\delta_m}}$, $x = 1$ and $n = 1$, we obtain

$$\zeta(s,\alpha_m) = s^{\delta_m}\sum_{k=0}^{\infty}\int_{s^{-\delta_m}}^{\infty}(-1)^k\frac{(1)_k}{k!}\, u^{-\frac{(k+1)}{\delta_m}} du \tag{33}$$

where $(x)_k = \frac{\Gamma(x+k)}{\Gamma(x)} = x(x+1)...(x+k-1)$, is the Pochhammer symbol [39], and we used the property $(1)_k = k!$. Evaluating the integral in (33) we obtain

$$\begin{aligned}\zeta(s,\alpha_m) =& s^{\delta_m}\sum_{k=0}^{\infty}(-1)^k\frac{(1)_k}{k!}\,\frac{s^{k-\delta_m+1}}{\frac{k+1}{\delta_m}-1} \\ =& s\,\delta_m\sum_{k=0}^{\infty}\frac{(1)_k}{k-\delta_m+1}\,\frac{(-s)^k}{k!}. \end{aligned} \tag{34}$$

By noting that $\frac{(x)_k}{(x+1)_k} = \frac{x}{x+k}$, with $x = 1-\delta_m$, then (34) can be expressed as

$$\zeta(s,\alpha_m) = \frac{s\,\delta_m}{1-\delta_m}\sum_{k=0}^{\infty}\frac{(1)_k(1-\delta_m)}{k-\delta_m+1}\,\frac{(-s)^k}{k!} \tag{35}$$

The summation in (35) corresponds to the general expression of the hypergeometric function given by ${}_2F_1(a,b;c;x) = \sum\limits_{k=0}^{\infty}\frac{(a)_k(b)_k}{(c)_k}\,\frac{(x)^k}{k!}$, and so using this expression and substituting (35) into (31), we obtain

$$\mathcal{K}_m(s, R_m) = E_{R_m}\left[e^{\frac{-\lambda_m \pi R_m^2\, s\,\delta_m}{N_S(1-\delta_m)}\,{}_2F_1(1,1-\delta_m;2-\delta_m;-s)}\right]. \tag{36}$$

Now, as previously stated, R_m is a random variable following the distribution of the closest neighbour, so obtaining the expected value in (36) with respect to the closest neighbour, yields

$$\begin{aligned}&\mathcal{K}_m(s, R_m) = E_{R_m}\left[\exp\left(\tfrac{-\lambda_m \pi R_m^2}{N_S}\,\zeta(s,\alpha_m)\right)\right] \\ &= \int_0^{\infty} 2\lambda_m \pi R_m\left(e^{-\frac{\lambda_m \pi R_m^2}{N_S}\,\zeta(s,\alpha_m)}\, e^{-\lambda_m \pi R_m^2}\right) dR_m \\ &= \tfrac{1}{1+\frac{\zeta(s,\alpha_m)}{N_S}} \\ &= \left(1+\tfrac{s\,\delta_m}{N_S(1-\delta_m)}\,{}_2F_1(1,1-\delta_m;2-\delta_m;-s)\right)^{-1} \end{aligned} \tag{37}$$

This concludes the evaluation of $\mathcal{K}_i(s, R_i)$).

REFERENCES

[1] Z. Hasan, H. Boostanimehr, and V. K. Bhargava, "Green cellular networks: A survey, some research issues and challenges," *IEEE Communications Surveys and Tutorials*, vol. 13, no. 4, pp. 524 – 540, 2011.

[2] A. Damnjanovi, J. Montojo, Y. Wei, T. Ji, T. Luo, M. Vajapeyam, T. Yoo, O. Song, and D. Malladi, "A survey on 3gpp heterogeneous networks," *IEEE Wireless Communications*, vol. 18, no. 3, pp. 10 – 21, June 2011.

[3] S. Cui, A. J. Goldsmith, and A. Bahai, "Energy-efficiency of mimo and cooperative mimo techniques in sensor networks," *IEEE Journal on Selected Areas in Communications*, vol. 22, no. 6, pp. 1089 – 1098, August 2004.

[4] D. Feng, G. Lim, L. J. Cimini, G. Feng, and G. Y. Li, "A survey of energy-efficient wireless communications," *IEEE Communications Surveys and Tutorials*, pp. 1 – 12, 2012.

[5] W. C. Cheung, T. Q. S. Quek, and M. Kountouris, "Throughput optimization, spectrum allocation, and access control in two-tier femtocell networks," *IEEE Journal on Selected Areas in Communications*, vol. 30, no. 3, pp. 561 –574, April 2012.

[6] T. Nakamura, S. Nagata, A. Benjebbour, Y. Kishiyama, T. Hai, S. Xiaodong, Y. Ning, and L. Nan, "Trends in small cell enhancements in lte advanced," *Communications Magazine, IEEE*, vol. 51, no. 2, pp. 98–105, 2013.

[7] D. Stoyan, W. S. Kendall, and J. Mecke, *Stochastic Geometry and Its Applications*, 2nd ed. WILEY, 1995.

[8] F. Baccelli, B. Blaszczyszyn, and P. Muhlethaler, "Stochastic analysis of spatial and opportunistic aloha," *IEEE Journal on Selected Areas in Communications*, vol. 27, no. 7, pp. 1105 – 1119, September 2009.

[9] S. Weber, J. G. Andrews, and N. Jindal, "The effect of fading, channel inversion, and threshold scheduling on ad hoc networks," *IEEE Transactions on Information Theory*, vol. 53, no. 11, pp. 4127 – 4149, November 2007.

[10] S. A. R. Zaidi, M. Ghogho, D. C. McLernon, and A. Swami, "Energy efficiency in large scale interference limited wireless ad hoc networks," *WCNC Workshop on Future Green Communications*, pp. 24 – 29, April 2012.

[11] V. Chandrasekhar and J. G. Andrews, "Spectrum allocation in tiered networks," *IEEE Transactions on Communications*, vol. 57, no. 10, pp. 3059 – 3068, October 2009.

[12] M. Wildemeersch, T. Q. S. Quek, C. H. Slump, and A. Rabbachin, "Cognitive small cell networks: Energy efficiency and trade-offs," *IEEE Transactions on Communications*, 2013.

[13] T. M. Nguyen, Y. Jeong, T. Q. S. Quek, W. P. Tay, and H. Shin, "Interference alignment in a poisson field of mimo femtocells," *IEEE Transactions on Wireless Communications*, vol. 12, no. 12, pp. 2633–2645, June 2013.

[14] T. M. Nguyen, H. Shin, and T. Q. S. Quek, "Network throughput and energy efficiency in mimo femtocells," *European Wireless Conference*, pp. 1 – 5, April 2012.

[15] J. G. Andrews, F. Baccelli, and R. Krishna, "A tractable approach to coverage and rate in cellular networks," *IEEE Transactions on Communications*, vol. 59, no. 11, pp. 3122 – 3134, November 2011.

[16] H. S. Dhillon, R. Krishna, F. Baccelli, and J. G. Andrews, "Modeling and analysis of k-tier downlink heterogeneous cellular networks," *Journal on Selected Areas in Communications*, vol. 30, no. 3, pp. 550 – 560, April 2012.

[17] A. M. Hunter, J. G. Andrews, and S. Weber, "Transmission capacity of ad hoc networks with spatial diversity," *IEEE Transactions on Wireless Communications*, vol. 7, no. 12, pp. 5058 – 5071, December 2008.

[18] A. J. Fehske, F. Richter, and G. P. Fettweiss, "Energy efficiency improvements through micro sites in cellular mobile radio networks," *GLOBECOM Workshops*, pp. 1 – 5, November 2009.

[19] H. Klessig, A. J. Fehske, and G. Fettweis, "Energy efficiency gains in interference-limited heterogeneous cellular mobile radio networks with random micro site deployment," *IEEE Sarnoff Symposium*, pp. 1 – 6, May 2011.

[20] F. Cao and Z. Fan, "The tradeoff between energy efficiency and system performance of femtocell deployment," *International Symposium on Wireless Communication Systems*, pp. 315 – 319, September 2010.

[21] T. Q. S. Quek, W. C. Cheung, and M. Kountouris, "Energy efficiency analysis of two-tier heterogeneous networks," *Wireless Conference - Suistainable Wireless Technologies*, pp. 1 – 5, April 2011.

[22] J. Rao and A. O. Fapojuwo, "Energy efficiency of outage constrainted two-tier heterogeneous cellular networks," *IEEE Wireless Communications and Networking Conference (WCNC)*, pp. 146–151, 2013.

[23] R. Hernandez-Aquino, D. McLernon, M. Ghogho, and S. A. R. Zaidi, "Energy efficiency in mimo large scale two-tier networks with beamforming and adaptive modulation," in *Signal Processing Conference (EUSIPCO), 2013 Proceedings of the 21st European*. IEEE, 2013, pp. 1–5.

[24] F. Héliot, M. A. Imran, and R. Tafazolli, "On the energy efficiency-spectral efficiency trade-off over the mimo rayleigh fading channel," *Communications, IEEE Transactions on*, vol. 60, no. 5, pp. 1345–1356, 2012.

[25] S. A. R. Zaidi, M. Ghogho, and D. C. McLernon, "Achievable spatial throughput in multi-antenna cognitive underlay networks with multi-hop relaying," *IEEE Journal on Selected Areas in Communications*, pp. 1 – 16, 2012.

[26] 3GPP, "TR36.814 v9.0.0.: Further advancements for E-UTRA physical layers aspects (release 9)," 3GPP, Technical Report, March 2010.

[27] V. Chandrasekhar, J. G. Andrews, and A. Gatherer, "Femtocell networks: a survey," *IEEE Communications Magazine*, vol. 46, pp. 59 – 67, 2008.

[28] Z. Chen, C.-X. Wang, X. Hong, J. S. Thompson, S. A. Vorobyov, X. Ge, H. Xiao, and F. Zhao, "Aggregate interference modeling in cognitive radio networks with power and contention control," *IEEE Transactions on Communications*, vol. 60, no. 2, pp. 456–468, February 2012.

[29] M. Haenggi, "Mean interference in hard-core wireless networks," *IEEE Communications Letters*, vol. 15, no. 8, pp. 792–794, August 2011.

[30] E.C.R., "Energy efficiency for network equipment: Two steps beyond greenwashing," Energy Consumption Rating Initiative, Tech. Rep., August 2008.

[31] M. Deruyck, D. D. Vulder, W. Joseph, and L. Martens, "Modelling the power consumption in femtocell networks," *WCNC Workshop on Future Green Communications*, pp. 30 – 35, April 2012.

[32] A. Goldsmith, *Wireless Communications*. 40 West 20th Street, New York: Cambridge University Press, 2005.

[33] A. J. Grant, "Performance analysis of transmit beamforming," *IEEE Transactions on Communications*, vol. 53, no. 4, pp. 738 – 744, April 2005.

[34] C. Khatri, "Distribution of the largest or the smallest characteristic root under null hypothesis concerning complex multivariate normal populations," *The Annals of Mathematical Statistics*, vol. 35, no. 4, pp. 1807 – 1810, 1964.

[35] F. Richter, A. J. Fehske, and G. P. Fettweis, "Energy efficiency aspects of base station deployment strategies for cellular networks," *IEEE Vehicular Technology Conference*, pp. 1 – 5, September 2009.

[36] Y. S. Soh, T. Q. S. Quek, M. Kountouris, and H. Shin, "Energy efficient heterogeneous cellular networks," *IEEE Journal on Selected Areas in Communications*, vol. 31, no. 5, pp. 840–850, May 2013.

[37] W. Cheng, H. Zhang, L. Zhao, and Y. Li, "Energy efficient spectrum allocation for green radio in two-tier cellular networks," *Global Telecommunications Conference (GLOBECOM 2010)*, pp. 1 – 5, December 2010.

[38] D. Halperin, B. Greenstein, A. Sheth, and D. Wetherall, "Demystifying 802.11n power consumption," *Proceedings of the 2010 international conference on Power aware computing and systems*, pp. 1 – 5, October 2010.

[39] I. Gradshteyn and I. Ryzhik, *Table of Integrals, Series, and Products*, 7th ed., A. Jeffrey and D. Zwillinger, Eds. MA, USA: Elsevier Academic Press, 2007.

Raul Hernandez-Aquino received the Electronic and Communications Engineer degree from Universidad De Las Americas (UDLAP) Puebla in May 2008. He graduated CUM LAUDE. During the following months, he worked as a Research Engineer at Instituto Nacional de Astrofisica, Optica y Electronica (INAOE) in Mexico. In 2008 he was an attendant to the Information and Communication Technology formation program of T-Systems Mexico, in Puebla where he received 5 certifications as server administrator (from Microsoft and Sun Microsystems). He worked as a System Administrator at T-Systems Mexico, from February to December 2009. On December 2012 he received his M.Sc. in electronics (major in Telecommunications) from Instituto Tecnologico y de Estudios Superiores de Monterrey (ITESM), in Mexico. He is currently pursuing a Ph.D. in Telecommunications at University of Leeds, UK. He is also a co-author of the "network management and traffic engineering" chapter of the book *Building Next-Generation Converged Networks: Theory and Practice* (Taylor and Francis, 2013). His research interests include broadly communication theory, heterogeneous networks, and signal processing for communications.

Syed Ali Raza Zaidi (M09) is currently a Research Fellow at the University of Leeds on the US Army Research Lab funded project. He received his B.Eng degree in information and communication system engineering from the School of Electronics and Electrical Engineering, NUST, Pakistan in 2008. He was awarded the NUSTs most prestigious Rectors gold medal for his final year project. From September 2007 till August 2008, he served as a Research Assistant in Wireless Sensor Network Lab on a collaborative research project between NUST, Pakistan and Ajou University, South Korea. In 2008, he was awarded overseas research student scholarship along with Tetley Lupton and Excellence Scholarships to pursue his PhD at the School of Electronics and Electrical Engineering, University of Leeds, U.K. He was also awarded with COST IC0902, DAAD and Royal Academy of Engineering grants to promote his research. Dr. Zaidi was a visiting research scientist at Qatar Innovations and Mobility Centre from October to December 2013. He has served as an invited reviewer for IEEE flagship journals and conferences. His research is focused towards design and analysis of the large scale ad-hoc wireless networks by employing tools from stochastic geometry and random graph theory. Dr. Zaidi is also UK Liasion for the European Association for Signal Processing (EURASIP). He has served on the program committees and as a chair in various IEEE flagship conferences. He is the technical program chair for EAI STEMCOM 2016 and workshop chair for the IEEE CAMAD 2015 special session on Performance Analysis and Modelling of Large-scale 5G networks, IEEE WCMC 2015 workshop on 'Recent Advances at Physical Layer for 5G Wireless Networks' and IEEE VTC workshop on 'Emerging device centric communication'. He has also served as a track chair for 'Theory and modeling track' at IEEE/ICST CROWNCOM 2015. Dr. Zaidi is also a Lead Guest Editor for IET Signal Processing SI on Recent Advances in Signal Processing for 5G Wireless Networks and associate editor for IEEE Communication Letters.

Des McLernon (M94) received his B.Sc in electronic and electrical engineering and his M.Sc. in electronics, both from Queens University of Belfast,N. Ireland. He then worked on radar research and development with Ferranti Ltd. in Edinburgh, Scotland, and later joined the Imperial College, University of London, where he received his Ph.D.in signal processing. After rst lecturing at South Bank University, London, UK, he moved to the School of Electronic and Electrical Engineering at the University of Leeds, UK, where he is a Reader in Signal Processing and Director of Graduate Studies. His research interests are broadly within the domain of signal processing for communications, in which area he has published over 280 journal and conference papers.

Mounir Ghogho (SM96) received the MSc degree (DEA) in 1993 and the PhD degree in 1997 from the National Polytechnic Institute of Toulouse, France. He was an EPSRC Research Fellow with the University of Strathclyde, Glasgow (Scotland), from September 1997 to November 2001. Since December 2001, he has been a faculty member with the school of Electronic and Electrical Engineering at the University of Leeds (UK), where he currently holds a Chair in Signal Processing and Communications. Since 2010, he has also been a Research Director at the International University of Rabat (Morocco). He is currently an Associate Editor of the IEEE Signal Processing magazine. He served as an Associate Editor of the IEEE Transactions on Signal Processing from 2005 to 2008, the IEEE Signal Processing Letters from 2001 to 2004, and the Elsevier Digital Signal Processing journal from 2011 to 2012. He is currently a member of the IEEE Signal Processing Society SAM Technical Committee. He served as a member of the IEEE Signal Processing Society SPCOM Technical Committee from 2005 to 2010 and a member of IEEE Signal Processing Society SPTM Technical Committee from 2006 to 2011. He was the General Chair of the eleventh IEEE workshop on Signal Processing for Advanced Wireless Communications (SPAWC2010), General Chair of the 21st edition of the European Signal Processing Conference (EUSIPCO 2013), the Technical co-Chair of the MIMO symposium of IWCMC 2007 and IWCMC 2008. His research interests are in signal processing and communication networks. He has published over 250 journal and conferences papers. He held invited scientist/professor positions at many institutions including the US Army Research Lab (USA), Tlcom Paris-Tech (France), National Institute of Informatics (Japan), the University Carlos Third of Madrid (Spain), ENSICA (France), Technical University of Darmstadt (Germany), the University of Minnesota (USA), Beijing University of Posts and Telecommunication (China), and the University Mohamed V (Morocco). He is the EURASIP Liaison in Morocco. He was awarded the UK Royal Academy of Engineering Research Fellowship in September 2000. He is also one of the recipients of the 2013 IBM Faculty award.